Positive Charge Carriers on Isolated Chains of MEH−PPV with Broken Conjugation: Optical Absorption and Mobility

Luis P. Candeias,*,† Ferdinand C. Grozema,† G. Padmanaban,‡ S. Ramakrishnan,‡ Laurens D. A. Siebbeles,† and John M. Warman†

Department of Radiation Chemistry, IRI, Delft University of Technology, Mekelweg 15, 2629 JB Delft, The Netherlands, and Department of Inorganic and Physical Chemistry, Indian Institute of Science, Bangalore 560 012, India

Received: July 18, 2002; In Final Form: November 15, 2002

Pulse radiolysis of oxygen-saturated dilute solutions of *poly*[2-methoxy-5-(2′-ethylhexyloxy)-1,4-phenylene vinylene]s in benzene showed charge-transfer from the solvent radical cation to the polymer, yielding positive charge carriers (radical-cations or "holes") on the isolated chains. The charge-transfer reactions are diffusion controlled with (time-dependent) rate coefficients that are determined by the conformation adopted by the polymer chains. The radical cation of the fully conjugated polymer exhibited an absorption maximum at 1.32 eV. The absorption maximum shifted to higher energies with decreasing conjugated fraction, in a way consistent with thermal equilibration of the positive charge over the conjugated segments of different length. The mobility of the positive charge along the fully conjugated MEH−PPV chains was determined to be 0.42 $cm^2\ V^{-1}\ s^{-1}$. The introduction of conjugated breaks decreased the charge mobility strongly, which is attributed to the disruption of the π conjugation and/or the conformational disorder caused by the flexibility of the chains at the sites of conjugation breaks.

Introduction

Poly(phenylene vinylene)s are a class of luminescent, conjugated polymers with potential applications in organic electrooptical devices.[1] The investigation of the properties of the charge carriers on the polymer chains is not only of practical relevance but has also raised interesting, fundamental questions, such as how the optical absorption and charge-transport properties of a chain depend on the conjugation length and backbone flexibility.

Recently, two of us (G.P. and S.R.) have prepared *poly*[2-methoxy-5-(2′-ethylhexyloxy)-1,4-phenylene vinylene]s in which a controlled fraction of the vinylene groups have been saturated, generating soluble polymer chains with a conjugated fraction *x* MEH−PPV−(*x*) (Figure 1).[2] The saturated C−C bonds decrease the conjugation length, block triplet energy transfer along the polymer chains,[3] and increase the chain flexibility.

In the present study, we have investigated the effect of these conjugation breaks on the optical properties and mobility of the positive charge carriers on isolated chains of MEH−PPV−(*x*) in dilute solution. The method used was pulse radiolysis with two detection techniques: time-resolved UV/VIS/NIR spectroscopy and time-resolved microwave conductivity (TRMC).[3−6] Pulses of high-energy electrons were used to generate charge carriers, and the optical properties, kinetics of formation and decay, and mobility of the charge carriers were investigated.

Experimental Section

The polymers used MEH−PPV−(*x*) had conjugated fractions *x* between 0.2 and 1. It should be noted that because of chemical damage during synthesis and handling the "fully conjugated" polymer may contain up to 2% of conjugation breaks ($x \geq 0.98$). The molecular weight of the polymers was 220−260 kDa, corresponding to ca. 1000 monomer units per chain.[2] Dilute solutions (typically 0.2 to 1 μM) of MEH−PPV−(*x*) in UV-spectroscopic grade benzene were freshly prepared before each experiment and were bubbled with benzene-saturated oxygen for at least 10 min. All experiments were performed at room temperature.

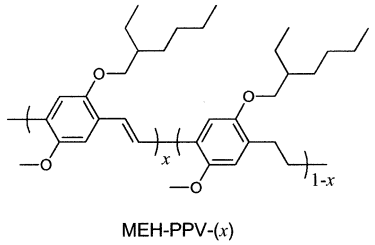

MEH-PPV-(*x*)

Figure 1. Molecular structures of the broken conjugation MEH−PPV polymers with conjugated fraction *x*.

The pulse radiolysis methods using time-resolved microwave conductivity (TRMC) or transient optical absorption detection were essentially as described previously.[4,6] In these techniques, the samples are irradiated with pulses of high-energy electrons, which generate charged and excited states. The amount of these species is proportional to the radiation dose deposited in the sample, usually expressed in gray ($1\ Gy = 1\ J\ kg^{-1}$). The ratio between the concentration of the primary species and the absorbed dose is the radiation-chemical yield, expressed in mol J^{-1} (or in number of ions or excited-states per 100 eV). Radiation-chemical yields for a variety of systems have been measured.

In our experimental setup, a Van de Graaff accelerator is used to generate 0.2−50 ns pulses of 3 MeV electrons. For the optical

* To whom correspondence should be addressed. Fax: +31-15-278 74 21. E-mail: candeias@iri.tudelft.nl.
† Delft University of Technology.
‡ Indian Institute of Science.

10.1021/jp021656c CCC: $25.00
Published on Web 01/24/2003

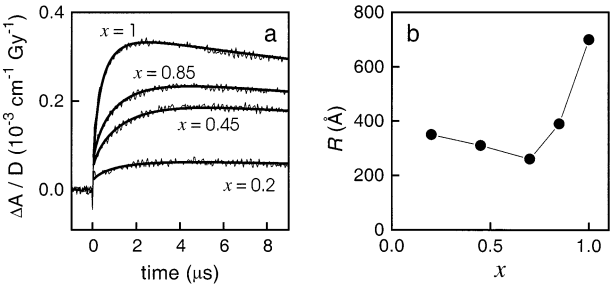

Figure 2. a: Formation of MEH−PPV−$(x)^{\bullet+}$, monitored by the dose-normalized optical absorption at the maximum, for polymer concentration 10^{-6} M and dose per pulse 20 Gy. The smooth lines are fits using a time-dependent rate coefficient as described in the text. b: Variation of the polymer effective radius (R) with conjugated fraction, determined from the fits.

absorption experiments, the dose per pulse (20 to 250 Gy) was calibrated using the aqueous electron dosimeter.[7] The solutions were flowed through the quartz cell (optical path 1.2 cm) by a slight overpressure of benzene-saturated oxygen. The source of detection light was a pulsed high-pressure Xe-lamp (450 W). Cutoff filters and a fast shutter were used to minimize photolysis of the solution by the detection light. NIR detection was achieved with a short-wavelength enhanced InGaAs photodiode (Hamamatsu, Japan). The transients were recorded by a Tektronix TDS680 digitizer.

For the TRMC measurements, the solutions were contained in a gold-coated Q-band microwave cell. They were first degassed by freeze−pump−thaw cycles on a vacuum line and then saturated with oxygen and sealed. Dosimetry was performed using radiochromic films.[4] The dose per pulse was varied between 4 and 40 Gy. The transients were recorded on a logarithmic time-scale using a Tektronix RTD 710 digitizer.

Results and Discussion

(i) Absorption Spectra of MEH−PPV−(x) Radical Cations. Irradiation of benzene (bz) generates radical cations ($bz^{\bullet+}$), excited states (bz*), and excess electrons (e_{bz}^-) (eq 1):[8]

$$bz \rightarrow bz^{\bullet+}, bz^*, e_{bz}^- \quad (1)$$

In pure benzene, these primary radiolysis products react with each other or with parent benzene. However, in the presence of other molecules and at low radiation doses, reaction of the primary products with those molecules prevails. For example, in oxygen-saturated benzene ($[O_2] = 11.9$ mM at 1 atm and 25 °C), the excited states and the excess electrons are rapidly scavenged within a few nanoseconds (eqs 2 and 3),[9] whereas the benzene radical cations are not affected:

$$bz^* + O_2 \rightarrow bz + {}^1O_2 \quad (2)$$

$$e_{bz}^- + O_2 \rightarrow O_2^{\bullet-} \quad (3)$$

Pulse radiolysis of MEH−PPV−(x) solutions in oxygen-saturated benzene resulted in absorptions in the range 0.9−2.2 eV which grew in after the pulse on a time-scale of microseconds (Figure 2a). The growth rate increased with increasing polymer concentration. In an experiment with the fully conjugated polymer MEH−PPV−(1), a concomitant decrease of absorbance in the same time domain was observed at 2.5 eV (500 nm), where the polymer absorbs. These results show that the absorbance changes are due to the reaction of a primary species produced in benzene (eq 1) with MEH−PPV−(x). On the basis of these results and considering the scavenging effect of oxygen on the excited states and excess electrons (eqs 2 and 3), the absorbance changes are attributed to the transfer of positive charge from the benzene radical cations to MEH−PPV−(x), yielding polymer radical-cations, MEH−PPV−$(x)^{\bullet+}$ (eq 4):

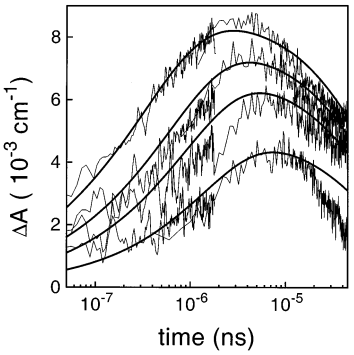

Figure 3. Transient absorption at 1.3 eV measured by pulse radiolysis of solutions of fully conjugated MEH−PPV in O_2 saturated benzene after 20 Gy pulses. The polymer concentrations, from the lowest to the highest curve, were 2×10^{-7}, 4×10^{-7}, 6×10^{-7}, and 1×10^{-6} M. The smooth lines are numerical fits based on the reaction mechanism described in the text.

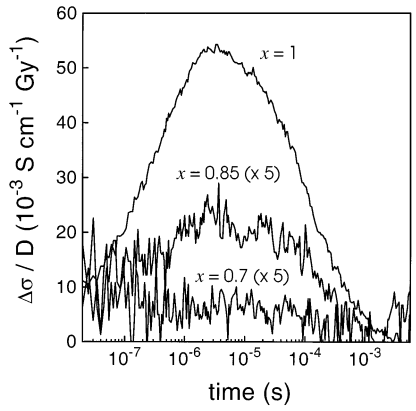

Figure 4. Dose-normalized transient conductivity observed on pulse radiolysis of solutions of MEH−PPV−(x) (10^{-6} M) in O_2-saturated benzene, after pulses of 20 Gy. The transients for $x = 0.85$ and 0.7 have been multiplied by a factor of 5.

$$bz^{\bullet+} + \text{MEH−PPV−}(x) \rightarrow bz + \text{MEH−PPV−}(x)^{\bullet+} \quad (4)$$

To verify this assignment, similar experiments were performed with solutions containing triethylamine (0.07 M), a well-known radical-cation scavenger. Under these conditions, the absorbance changes were suppressed, showing that they were due to the formation of MEH−PPV−$(x)^{\bullet+}$. Additional evidence was provided by the TRMC experiments (see below), which show the production of mobile, charged species with the same growth kinetics as the optical absorption (cf. Figures 3 and 4).

The absorption spectra of MEH−PPV−$(x)^{\bullet+}$ were obtained by measuring the transient changes of absorbance at different photon energies (Figure 5). The energies of the absorption maxima (Table 1) showed a systematic blue shift with decreasing conjugated fraction.

For the fully conjugated polymer, the spectrum of the radical cation was the same as that previously obtained in chloroform solution.[10] The radical-cation absorption at energies lower than that of the neutral molecule has been attributed to transitions involving two polaronic states, POL1 and POL2, lying in the gap between the valence and conduction bands (Figure 6).[11]

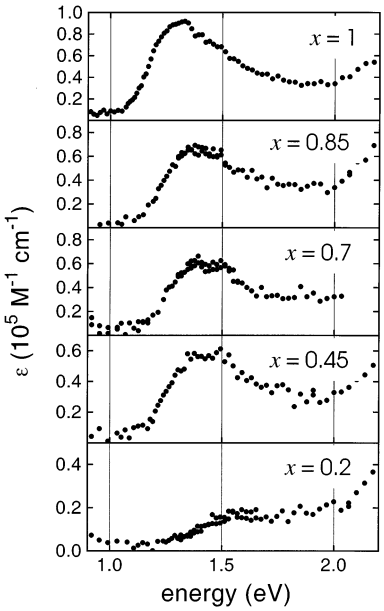

Figure 5. Absorption spectra of the MEH−PPV-(*x*) radical cations (conjugated fraction *x* given in the figure).

TABLE 1: Spectral Properties, Effective Radius (*R*), and Charge Mobility (μ^{+}_{1D}) of the MEH−PPV−(*x*) Radical Cations

x	ΔE_{max}/eV[a]	$\epsilon/10^5$ M^{-1} cm^{-1}[b]	*R*/Å[c]	μ^{+}_{1D}/cm^2 V^{-1} s^{-1}[c]
0.2	1.60	0.18	350	
0.45	1.47	0.55	310	<0.005
0.7	1.44	0.63	260	≈0.01
0.85	1.40	0.66	390	0.04
1	1.32	0.92	700	0.42

[a] ±0.01 eV. [b] ±10^3 M^{-1} cm^{-1}. [c] From the fitting procedure described in the text; uncertainty ca. 20%.

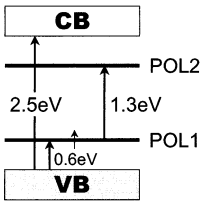

Figure 6. Energy levels of MEH−PPV$^{\bullet+}$ in the approximate band formalism. VB, valence band; CB, conduction band; POL1 and POL2, polaron levels. Allowed transitions and their energies are shown. (The short arrow indicates the unpaired electron on POL1.)

According to this interpretation, the absorption band observed here with $\Delta E = 1.3$ eV corresponds (mainly) to the POL1 → POL2 transition. Two other absorption bands are predicted, one overlapping the parent absorption at ca. 2.5 eV and another at ca. 0.6 eV [= (2.5−1.3)/2], which is outside the detection range of our equipment. The fact that a decrease of absorption was observed at 2.5 eV indicates that the extinction coefficient of the radical-cation for this transition is less than for the band-gap transition in the neutral molecule (ca. 1.5×10^4 M^{-1} cm^{-1}).

The absorption maxima of the radical cations of oligomers of phenylene vinylene have been found to shift to higher energies with decreasing chain length.[12] This chain length effect can partially explain the observed shift of the absorption maximum of MEH−PPV−(*x*)$^{\bullet+}$ to higher energies with decreasing *x*. These polymers consist of a distribution of conjugated segments of *n* consecutive phenylene vinylene (PV) units, separated by broken conjugation sites (phenylene ethylidine units). As discussed in the following paragraphs, the distribution

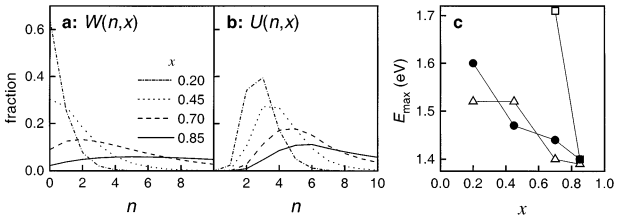

Figure 7. Distribution of positive charges over conjugated segments of length *n* calculated by (a) the mass-weighted distribution *W*(*n*,*x*) and (b) Boltzmann distribution *U*(*n*,*x*). Panel c shows the energy of the maxima of the optical absorption obtained from *W*(*n*,*x*) (open squares), from *U*(*n*,*x*) (open triangles), and measured experimentally (solid circles).

of the excess positive charge over the conjugated segments can be derived from statistical, kinetic, and thermodynamic arguments. On the basis of this distribution and the reported absorption spectra of PV oligomers,[12] the absorption maxima of MEH−PPV−(*x*)$^{\bullet+}$ can be predicted and compared with the experimentally measured values.

The probability *P*(*n*,*x*) of finding a segment of *n* consecutive PV units in a polymer of conjugated fraction *x* is given by eq 5:

$$P(n,x) = (1 - x)x^n \tag{5}$$

Assuming that the diffusion-controlled charge transfer from bz$^{\bullet+}$ to the polymer chain results in charges located with equal probability on conjugated and nonconjugated sites, the distribution of charge over conjugated segments of length *n* is proportional to the mass fraction of these segments *W*(*n*,*x*) (eq 6):

$$W(n,x) = (n + 1)(1 - x)^2x^n \tag{6}$$

The most probable conjugation lengths *n*, i.e. the maxima of *W*(*n*,*x*), for $x = 0.85$, $x = 0.7$, and $x \leq 0.45$ are 5, 2, and 0, respectively (Figure 7a). (Conjugation length 0 corresponds to the saturation of consecutive vinylene groups.) The radical cations of the PV oligomers of this length have absorption maxima at energies higher than experimentally measured (Figure 7c).

Alternatively, it maybe assumed that the excess charge rapidly reaches thermodynamic equilibrium. In this case, the energy-weighted charge distribution *U*(*n*,*x*) is given by a Boltzmann distribution (eq 7 and Figure 7b):

$$U(n, x) = P(n,x) \exp(-E_n/RT)/\sum [P(n,x) \exp(-E_n/RT)] \tag{7}$$

In eq 7, E_n is the energy of the charge on a segment of conjugated length *n*; the experimentally determined reduction potentials of the radical cations of PV oligomers are a measure of E_n.[12] (For $n = 0$, we used the reduction potential of the 1,4-dimethoxybenzene radical cation $E_0 = 1.34$ V vs SCE.) This method predicts absorption maxima of MEH−PPV−(*x*)$^{\bullet+}$ with a shallow dependence on the conjugated fraction, in agreement with the experimental observation (Figure 7c). This suggests that the excess charge is indeed thermodynamically equilibrated over the conjugated segments of different length and that the time scale for this equilibration is shorter than the time for the formation of charge transfer from bz$^{\bullet+}$ under the conditions of our experiments (≤3 μs).

(ii) Kinetics of Formation and Decay of MEH−PPV-*x* Radical Cations. The kinetics of formation of MEH−PPV−(1)$^{\bullet+}$ were monitored by transient absorbance at 1.3 eV and by

TRMC, using a low dose per pulse (20 Gy) and several polymer concentrations (0.2−1 μM). The two techniques gave the same results. The rate of formation k_{obs} estimated from an exponential fit to the growth of absorbance or conductivity, shows a supralinear dependence on the polymer concentration (not shown). This observation can be explained if reaction 4 is diffusion-controlled and with large reaction radius. In a detailed discussion of the kinetics of diffusion-controlled reactions, Noyes[13] predicted that the rate-coefficient k should be time-dependent and approximated by eq 8, where D is the sum of the diffusion coefficients of the reactants and R is the reaction radius:

$$k(t) = 4\pi RD[1 + R(\pi Dt)^{-1/2}] \quad (8)$$

The time required for the rate coefficient to differ by less than 10% from the value at long times ($4\pi RD$) is ca. 30 R^2/D. For reactions between small molecules with reaction radii of the order of 1 Å and diffusion coefficients of the order of 10^{-5} cm^2 s^{-1}, the rate coefficient differs less than 10% from the limiting long-time value after less than a nanosecond. In the present case of the reaction of bz$^{\bullet+}$ with MEH−PPV, D is essentially the diffusion coefficient of bz$^{\bullet+}$ ($D = 1.0 \times 10^{-5}$ cm^2 s^{-1}),[14] because the diffusion coefficient of the polymer is expected to be much smaller. On the other hand, the reaction radius R will be determined by the effective radius of the polymer chains. A value of R, of ca. 1000 Å, which seems reasonable for chains of ca. 1000 monomer units (see below), implies that it should take ca. 0.3 ms for the rate coefficient of reaction 4 to approach its limiting value. This is much longer than the time for completion of the formation of polymer cations in our experiments (cf. Figures 2a, 3, and 4). We have therefore observed reaction 4 in a regime of time-dependent rate coefficient. Indeed, using a time-dependent rate coefficient as given by eq 8 yielded good fits to the data (see below).

In further experiments with MEH−PPV−(1), it was observed that the absorbance at 1.3 eV or the transient conductivity measured after completion of the formation of MEH−PPV−(1)$^{\bullet+}$ increased with increasing polymer concentration and decreased with increasing dose per pulse. This can be ascribed to the competition between the charge-transfer from bz$^{\bullet+}$ to the polymer chains (eq 4) and the decay of bz$^{\bullet+}$ by reaction with $O_2^{\bullet-}$ (eq 9):

$$\text{bz}^{\bullet+} + O_2^{\bullet-} \rightarrow \text{products} \quad (9)$$

In experiments with the fully conjugated polymer, the lifetime of MEH−PPV−(1)$^{\bullet+}$(τ) was found to decrease with increasing dose per pulse, i.e., with the initial concentration of radical ions. This indicates that MEH−PPV−(x)$^{\bullet+}$ decays by a second-order process which we attribute to the recombination with $O_2^{\bullet-}$ (eq 10):

$$\text{MEH−PPV−}(x)^{\bullet+} + O_2^{\bullet-} \rightarrow \text{MEH−PPV−}(x) + O_2 \quad (10)$$

The rate coefficient of reaction 10, determined from the dependence of τ on the dose per pulse and the known yield of radicals (4.8×10^{-9} mol dm^{-3} Gy^{-1}),[15] was $k \approx 1 \times 10^{11}$ M^{-1} s^{-1}. No evidence was found for a concentration-independent decay process competing with reaction 10. This observation implies that for isolated molecules in solution positive charges are not trapped on the polymer chain and do not react with oxygen. Even in thin films, trapping of the positive charge carrier has been deemed insignificant.[16]

To confirm the proposed mechanism of formation and decay of MEH−PPV−(x)$^{\bullet+}$, a set of differential rate equations including the formation of MEH−PPV−(x)$^{\bullet+}$ by reaction 4 (with time-dependent rate coefficient given by eq 8), the competition by reaction 9, and the decay of MEH−PPV−(x)$^{\bullet+}$ by reaction 10 were solved numerically and fitted to the time-dependent absorbance at 1.3 eV measured experimentally with the fully conjugated polymer (Figure 3). Details of the numerical procedure will be published elsewhere.[17] From the fits, the extinction coefficient of MEH−PPV−(*1*)$^{\bullet+}$ at 1.3 eV was determined to be 9.0×10^4 M^{-1} cm^{-1}, which corresponds to an absorption cross-section of 3.4×10^{-16} cm^2. Integration of the absorption band yielded an oscillator strength of ca. 1.1.

The same numerical procedure was applied to fit the formation of the broken conjugation radical cations. The reaction radius (R) and the extinction coefficients of MEH−PPV−(x)$^{\bullet+}$ (ϵ) were used as adjustable parameters, whereas the initial yield and diffusion coefficient of bz$^{\bullet+}$ and the rate coefficients of reactions 9 and 10 were held constant. The extinction coefficients of the radical cations at the maxima obtained from the fitting procedure are listed in Table 1. They show a systematic decrease with the decreasing degree of conjugation. This observation can in part be explained by the distribution of charges over conjugated segments of different lengths discussed in the previous section. The fraction of charges localized on short conjugated segments increases with decreasing x; these charges have their absorption at high energies (VIS and UV) and do not contribute to the NIR absorption.

The reaction radii R obtained from the fits are also dependent on the conjugated fraction x (Figure 2b). The largest reaction radius ($R = 700$ Å) was obtained for the fully conjugated polymer; a small amount of conjugation breaks decreased R, but for $x < 0.7$, the reaction radius increased again slightly with increasing number of conjugation breaks (Figure 2b). This variation of R with conjugated fraction can be ascribed to the different conformations assumed by the polymer chains. The fully conjugated chain has a rigid, rodlike structure and hence a large effective radius. The introduction of a small number of saturated C−C bonds increases the chain flexibility at these points and allows the molecule to collapse into a toroidal conformation of smaller effective radius. The chains with small conjugated fractions ($x < 0.7$) are highly flexible and assume a random-coil structure, which has a radius between that of the toroidal and rodlike structures.[18]

(iii) Mobility of the Positive Charge on MEH−PPV-(x) Chains. To investigate the mobility of the positive charge along the broken conjugation chains, experiments with the MEH−PPV−(x) solutions were carried out using time-resolved microwave conductivity (TRMC). For the polymers with the highest conjugated fractions ($x \geq 0.7$), an increase of conductivity following the pulse was observed, followed by a decay (Figure 4), with the same kinetics as the formation and decay of MEH−PPV−(x)$^{\bullet+}$ under the same conditions of concentration and dose, as monitored by transient optical absorption. The conductivity increase shows that the transfer of the positive charge to the polymer chains on reaction of bz$^{\bullet+}$ with MEH−PPV−(x) results in an increase of the mobility; that is, the positive charge mobility along the polymer chains is higher than that of bz$^{\bullet+}$ itself. The one-dimensional mobility of the positive charges along the polymer chains $\mu_{1D}{}^+$ (in cm^2 V^{-1} s^{-1}) is related to the transient conductivity $\Delta\sigma$ (in S cm^{-1}) by eq 11, where e is the elementary charge (1.6×10^{-19} C) and $N_{\text{MEH−PPV+}}$ is the concentration of charge carriers on MEH−PPV chains (in charges/cm^3). The factor 1/3 converts the measured conductivity in randomly oriented polymer chains to the one-dimensional mobility.

$$\Delta\sigma = (1/3)eN_{\mathrm{MEH-PPV+}}\,\mu_{1\mathrm{D}}{}^{+} \qquad (11)$$

Using this equation, $\mu_{1D}{}^{+}$ can be calculated from the time-dependent MEH−PPV−$(x)^{\bullet+}$ concentration obtained from the kinetic fits to the transient absorption results described above. The values obtained (Table 1) show that conjugation breaks strongly decrease the mobility of the positive charge. A similar effect was previously observed in solid samples of related *poly*(phenylene vinylene)s.[19,20] Both electronic and steric reasons may lie behind the decrease of mobility with decreasing x: the saturated C−C bonds not only interrupt the π conjugation but their torsional freedom also introduces conformational disorder that decreases the charge mobility.

The high "hole" mobility measured for the fully conjugated polymer ($\mu_{1D}{}^{+} = 0.42$ cm^2 V^{-1} s^{-1}) demonstrates the remarkable conducting properties of the polymer chains. Previously, the sum of the mobilities of the positive and negative charges in a solid sample of MEH−PPV was measured by pulse radiolysis-TRMC, and a much lower value (ca. 10^{-3} cm^2 V^{-1} s^{-1}) was obtained.[21] The comparison of these results suggests that in the bulk solid the polymer chains are forced into conformations that are detrimental to charge migration. The positive charge mobility value obtained by current−voltage measurements on PPV-based devices is even lower (ca. 10^{-7}−10^{-5} cm^2 V^{-1} s^{-1}).[16,20,22] In this case, interchain charge transfer and the necessity for charge transfer across domain boundaries appear to have a further detrimental effect on charge transport through the bulk solid.

Acknowledgment. F.C.G. acknowledges the Priority Program for Materials research (PPM) of The Netherlands Organization for Scientific Research (NWO) for financial support.

References and Notes

(1) Burroughes, J. H.; Bradley, D. D. C.; Brown, A. R.; Matks, R. N.; Mackay, K.; Burns, P. L.; Holmes, A. B. *Nature* **1990**, *347*, 539−541. Friend, R. H.; Gymer, R. W.; Holmes, A. B.; Burroughes, J. H.; Marks, R. N.; Taliani, C.; Bradley, D. D. C.; dos Santos, D. A.; Brédas, J. L.; Lögdlund, M.; Salaneck, W. R. *Nature* **1999**, *397*, 121−128. Sirringhaus, H.; Tessler, N.; Friend, R. H. *Science* **1998**, *280*, 1741−1744.

(2) Padmanaban, G.; Ramakrishnan, S. *J. Am. Chem. Soc.* **2000**, *122*, 2244−2251.

(3) Candeias, L. P.; Padmanaban, G.; Ramakrishnan, S. *Chem. Phys. Lett.* **2001**, *349*, 394−398.

(4) Schouten, P. G.; Warman, J. M.; de Haas, M. P.; van Nostrum, C. F.; Gelinck, G. H.; Nolte, R. J. M.; Copyn, M. J.; Zwikker, J. W.; Engel, M. K.; Hanack, M.; Chang, Y. H.; Ford, W. T. *J. Am. Chem. Soc.* **1994**, *116*, 6880−6894.

(5) Hoofman, R. J. O. M.; de Haas, M.; Siebbeles, L. D. A.; Warman, J. M. *Nature* **1998**, *392*, 54−56. Grozema, F. C.; Siebbeles, L. D. A.; Warman, J. M.; Seki, S.; Tagawa, S.; Scherf, U. *Adv. Mater.* **2002**, *14*, 228−231.

(6) Candeias, L. P.; Wildeman, J.; Hadziioannou, G.; Warman, J. M. *J. Phys. Chem. B* **2000**, *104*, 8366−8371.

(7) Hart, E. J.; Fielden, E. M. The hydrated electron dosimeter. In *Manual of Radiation Dosimetry*; Holm, N. W., Berry, R. J., Eds.; Marcel Dekker: New York, 1970; pp 331−335.

(8) Cooper, R.; Thomas, J. K. *J. Chem. Phys.* **1968**, *48*, 5097−5102. Thomas, J. K.; Mani, I. *J. Chem. Phys.* **1969**, *51*, 1834−1838.

(9) Gorman, A. A.; Lovering, G.; Rodgers, M. A. J. *J. Am. Chem. Soc.* **1978**, *100*, 4527−4532.

(10) Burrows, H. D.; Miguel, M. G.; Monkman, A. P.; Horsburgh, L. E.; Hamblett, I.; Navaratnam, S. *J. Chem. Phys.* **2000**, *112*, 3082−3089.

(11) Cornil, J.; Belijonne, D.; Brédas, J. L. *J. Chem. Phys.* **1995**, *103*, 834−841.

(12) van Hal, P.; Beckers, E. H. A.; Peeters, E.; Apperloo, J. J.; Janssen, R. A. J. *Chem. Phys. Lett.* **2000**, *328*, 403−408.

(13) Noyes, R. M. *Prog. React. Kinet.* **1961**, *1*, 129−160.

(14) Huang, S. S. S.; Freeman, G. R. *J. Chem. Phys.* **1980**, *72*, 1989−1993.

(15) Gee, N.; Freeman, G. R. *Can. J. Chem.* **1992**, *70*, 1618−1622. Schmidt, W. F.; Allen, A. O. *J. Phys. Chem.* **1968**, *72*, 3730−3736.

(16) Bozano, L.; Carter, S. A.; Scott, J. C.; Malliaras, G. G.; Brock, P. J. *Appl. Phys. Lett.* **1999**, *74*, 1132−1134.

(17) Grozema, F. G.; Hoofman, R. J. O. M.; Candeias, L. P.; Siebbeles, L. D. A.; de Haas, M. P.; Warman, J. M. Manuscript in preparation.

(18) Hu, D.; Yu, J.; Wong, K.; Bagchi, B.; Rossky, P. J.; Barbara, P. F. *Nature* **2000**, *405*, 1030−1033.

(19) Gelinck, G. H.; Warman, J. M. *J. Phys. Chem.* **1996**, *100*, 20035−20042.

(20) Martens, H. C. F.; Blom, P. W. M.; Schoo, H. F. M. *Phys. Rev. B* **2001**, *61*, 7489−7493.

(21) Gelinck, G. H.; Warman, J. M.; Schoo, H. F. M. *J. Radioanal. Nucl. Chem.* **1998**, *232*, 115−119.

(22) Martens, H. C. F.; Brom, H. B.; Blom, P. W. M.; Schoo, H. F. M. *Phys. Stat. Sol. B* **2000**, *218*, 283−286.